

# Stress relaxation in precipitation-hardenable alloys

P. Buchhagen and W. Riehemann

Institut für Werkstoffkunde und Werkstofftechnik, Technische Universität Clausthal, Agricolastrasse 6, W-38678 Clausthal-Zellerfeld (Germany)

## Abstract

Sensitive stress relaxation measurements of the precipitation-hardenable alloys CuBe<sub>2</sub>, Nimonic PE16, Nimonic 105 and solid-solution Alloy 825 have been performed in order to minimize the relaxation effects. In all samples, part of the stress relaxation fades away after plastic deformation or heat treatment over several days. So the relaxation strength itself shows an effect of recovery. In CuBe<sub>2</sub> the change in stress relaxation can be explained because precipitates lower the free segment length of mobile dislocations and because of the depletion of Be solid solutes. At about 300 °C, ordering effects in the nickel alloys Nimonic PE16 and Alloy 825 correlate with stress relaxation. In Nimonic PE16 and Nimonic 105, precipitation occurs at 650 °C and 700 °C respectively and affects the stress relaxation strength. All effects including the slowly ascending stress relaxation curves can be explained by a dislocation mechanism with involved solid solutes.

## 1. Introduction

In various precision mechanical devices such as high resolution electrodynamic balances, engineering materials with a low stress relaxation strength are needed especially for spring applications. In order to obtain small spring constants, one has to choose small dimensions requiring a high yield strength. Precipitation hardening is known to be effective for the increase in yield strength, even at higher temperatures. Unfortunately very little is known about the effect of precipitates on stress relaxation and damping.

Therefore we measured the anelastic portion of the stress relaxation of copper–beryllium and nickel-based precipitation-hardenable alloys near room temperature. The samples have been subjected to various thermo-mechanical treatments in order to change the dislocation density and the degree of precipitation.

## 2. Experimental details

The stress relaxation was measured using electrodynamic balances [1, 2]. Their control circuits were modified in order to raise or lower the scale up to a maximum of 120  $\mu\text{m}$  by an external voltage. The specimens in the form of transverse beams were attached firmly to the balance on one side. A weight connected the free end of the beam to the scale. So the force of the weight was divided between the forces onto the scale and onto the beam. Via a personal computer

(PC) and digital-to-analogue converter the stroke of the scale loaded or unloaded the beam. The change in stress  $\sigma$  is proportional to the change in weight reading  $G$ . After a change in stress, the control circuit maintains a constant strain in the specimen. The resultant stress relaxation  $\Delta\sigma$  causes a change  $\Delta G(t)$  in the weight reading which was recorded by the PC. The reversible modulus defect  $(\Delta E/E)(t) = (\Delta\sigma/\sigma)(t) = (\Delta G/G)(t)$  was measured in a time ranging from 3 to 3030 s. For further details see refs. 1 and 2.

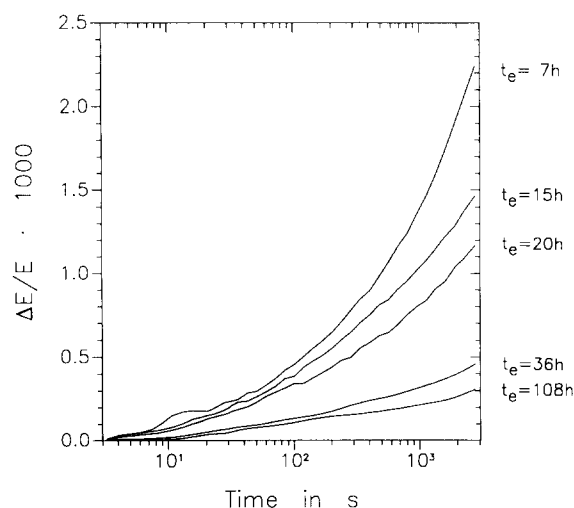


Fig. 1. Reversible modulus defect of CuBe<sub>2</sub> after heat treatment (250 °C for 1 h) vs. time on a logarithmic scale for various recovery times  $t_e$  at room temperature.

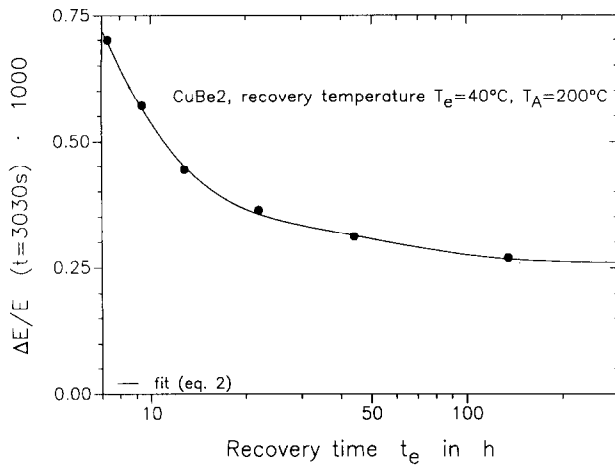


Fig. 2. Stress relaxation strength vs. recovery time after heat treatment (200 °C for 1 h), where  $\tau_1=4.2$  h and  $\tau_2=45$  h.

In order to examine the influence of precipitates on the stress relaxation behaviour the microstructure was varied by successive isochronal or isothermal heat treatments, which were carried out by stepwise increase in the temperature after aging for 1 h. After each temperature step of 50 °C the beam was quenched into water in order to measure the stress relaxation and the Vickers hardness.

### 3. Results and discussion

Copper-beryllium alloys are well-known materials for spring components with a high yield stress and a low

stress relaxation [3]. The examined alloy with 2 wt.% (12 at.%) Be can be hardened by precipitation. An increase in the Vickers hardness of about 300 HV 10 is possible by suitable aging of the supersaturated solid solution state. In CuBe<sub>2</sub>, three types of precipitate have been observed: Guinier-Preston (GP) zones, semicoherent interphase precipitates and incoherent  $\beta'$  particles, which precipitate discontinuously [3]. Their behaviour dependences on time and temperature are well known [4-6].

An example of the time dependence of stress relaxation in CuBe<sub>2</sub> after heat treatment is shown in Fig. 1. It is possible to describe the relaxation behaviour by only two parameters:

$$\frac{\Delta E(t)}{E} = K[t^n - (3s)^n] \quad (1)$$

where  $K$  is proportional to the relaxation strength, the mean segment length of pinned dislocations and the density of these segments [7]. The origin of the exponent  $n$  is the correction factor of the energy  $U$  occurring in the empirical temperature dependence of the high temperature background to its activation energy  $U_0$ , where  $U=nU_0$  [11]. For all measurements on CuBe<sub>2</sub>,  $n$  was in the range  $0.21 < n < 0.37$ .

After heat treatment there is a strong recovery in stress relaxation which fades away after a recovery time  $t_e$  of a few days. Owing to the similar time dependences of the relaxation in different samples with various microstructures it is possible to characterize the relaxation by  $(\Delta E/E)$  ( $t=3030$  s). The time dependence

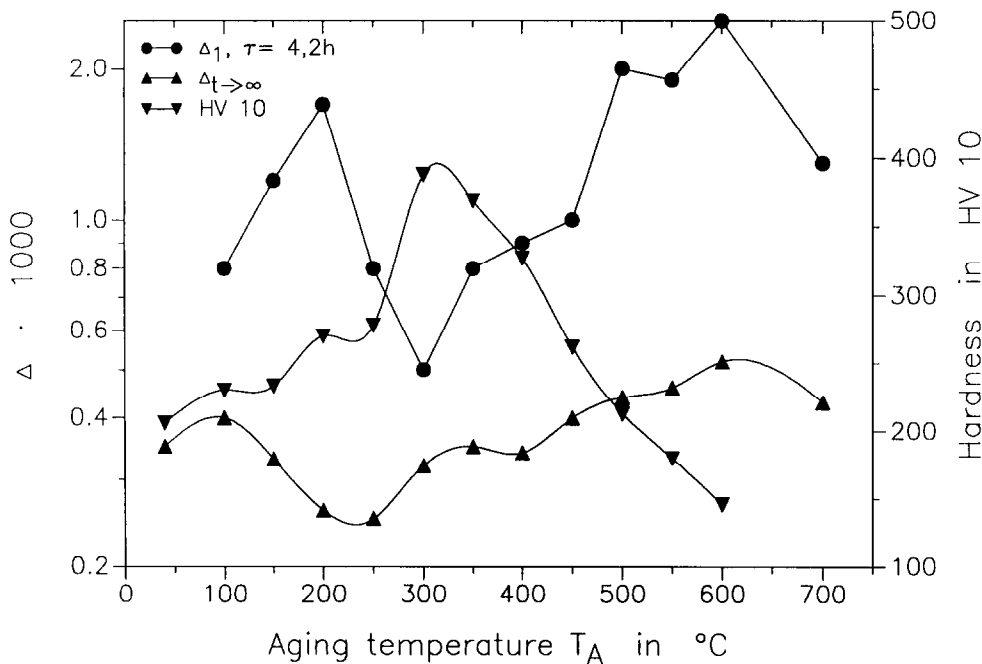


Fig. 3. Recovery strength  $\Delta_1$ , fully recovered stress relaxation strength  $\Delta_{t \rightarrow \infty}$  on a logarithmic scale and hardness vs. aging temperature of successive step-by-step isochronal heat treatments of a cold-worked CuBe<sub>2</sub> specimen.

of recovery (Fig. 2) can be described by

$$\frac{\Delta E(t)}{E}(t_e) = \Delta_1 \exp\left(-\frac{t_e}{\tau_1}\right) + \Delta_2 \exp\left(-\frac{t_e}{\tau_2}\right) + \Delta_{t \rightarrow \infty} \quad (2)$$

The recovery time constants  $\tau_1$  and  $\tau_2$  depend solely on the recovery temperature. On the assumption that a dislocation mechanism is responsible for the stress relaxation effect the recovery of the relaxation strength can be explained by pinning of the dislocations by solid solutes developing Cottrell or Suzuki clouds during aging at room temperature and higher temperatures.

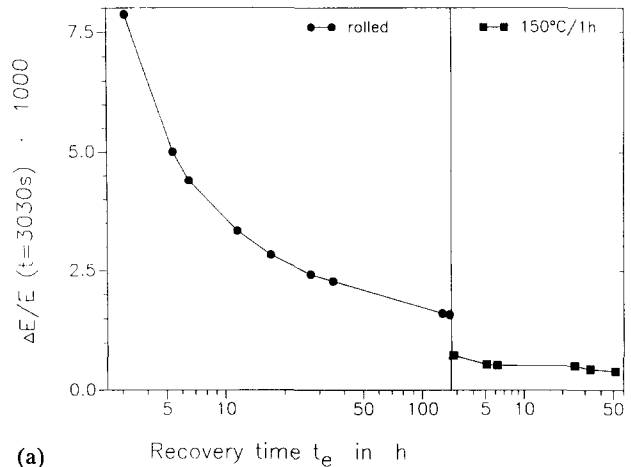
The recovery strength  $\Delta_1$ , the fully recovered stress relaxation  $\Delta_{t \rightarrow \infty}$  and the Vickers hardness (load, 10 kgf) of cold-worked CuBe2 are strongly dependent on the microstructure, changing with aging temperature  $T_A$  as can be seen in Fig. 3.

According to the literature [3] the aging temperature scale can be subdivided into four ranges. For  $T_A < 200$  °C the volume fraction of weakly hardening GP zones increases. Only a few interphase particles occur. For  $200$  °C  $< T_A < 300$  °C, GP zones transform into an interphase and finally into  $\beta'$  precipitates. For  $300$  °C  $< T_A < 600$  °C the strongly hardening discontinuous  $\beta'$  phase overages with increasing temperature. The  $\beta'$  volume fraction increases. For  $T_A > 600$  °C the  $\beta'$  phase dissolves in the matrix.

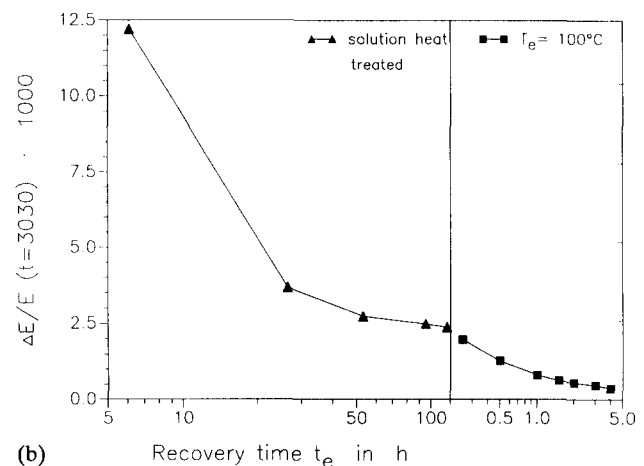
In Fig. 3(a) a maximum in the hardness and a minimum in the recovered relaxation strength can be observed. For a dislocation mechanism this has to be expected owing to a change in the pinning of the dislocations for various precipitates. However, the minimum of the fully recovered stress relaxation is completed even before the onset of the discontinuous  $\beta'$  precipitation while the maximum of hardness is reached at higher temperatures when most of the precipitates are  $\beta'$ . This could be due to the different stresses in hardness and relaxation measurements. Solute atoms as well as weak precipitates (in this case GP zones) with small distances suppress the bowing out of the dislocation segments more effectively at lower stress levels than strong pinning points with larger distances, which are needed to pin the dislocations at higher stress levels.

The small values of  $\Delta_1$  and  $\Delta_{t \rightarrow \infty}$  for high and low temperatures (solid-solution state) can be explained by a high concentration of solutes, leading to a fast development of clouds (low  $\Delta_1$ ) and more pinning on dislocations (low  $\Delta_{t \rightarrow \infty}$ ). The minimum of  $\Delta_1$  in the temperature region of peak hardening cannot be explained by simple arguments.

In order to obtain minimum relaxation strength, one has (starting from present considerations) to adjust the dispersion of  $\beta'$  precipitations to low distances at



(a)



(b)

Fig. 4. Stress relaxation strength of Nimonic PE16 vs. recovery time  $t_e$ . (a) Recovery at 20 °C after cold rolling (left) and after heat treatment (150 °C for 1 h) (right). (b) Recovery after solution heat treatment at 20 °C (left) and at 100 °C (right).

maximum volume fraction. This can be obtained by isothermal heat treatment at a low aging temperature. Indeed, no stress relaxation could be found within the accuracy of our measurement equipment after isothermal heat treatment at 315 °C for 4 h.

The isochronal heat treatment was repeated after a solution heat treatment. The curves of  $\Delta_1$ ,  $\Delta_{t \rightarrow \infty}$  and hardness are shifted to higher aging temperatures compared with the cold-formed initial state. The minimum at 300 °C is slightly lower. Although the higher dislocation density accelerates the precipitation behaviour, it hardly influences the stress relaxation strength.

The nickel-based alloys Nimonic PE16 (43Ni-16.7Cr-34Fe-1.1Al-1.3Ti-5.1Mo), Nimonic 105 (52Ni-15.3Cr-19.2Co-4.9Al-1.3Ti-5.1Mo) and Alloy 825 (40Ni-21Cr-33Fe-2.8Mo) (where the compositions are given in weight per cent) have been investigated in the same way as CuBe2. Nimonic PE16 and Nimonic 105 are hardenable by coherent  $\gamma'$  ( $\text{Ni}_3(\text{Ti}, \text{Al})$ ) particles, a long-range ordered phase in the f.c.c. matrix with a

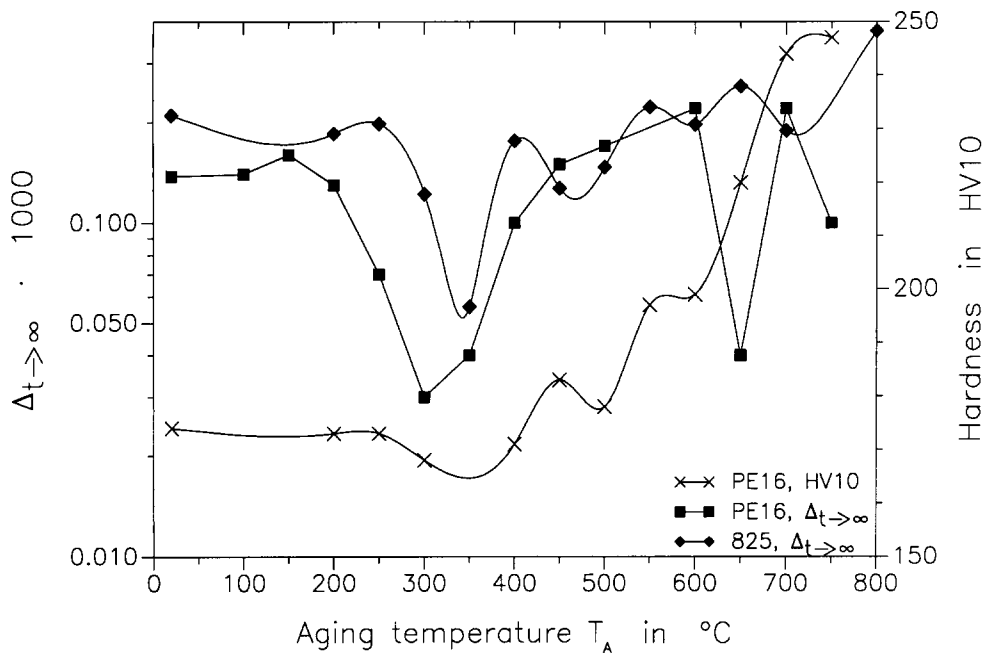


Fig. 5. Fully recovered relaxation strength  $\Delta_{t \rightarrow \infty}$  on a logarithmic scale and hardness *vs.* aging temperature for successive isochronal heat treatments of solution-treated specimens Nimonic PE16 and Alloy 825.

very small misfit [8] which is stable up to 900 °C for Nimonic PE16 and 1060 °C for Nimonic 105. In the temperature range 300–550 °C, ordered structures occur in the matrix for all investigated alloys [9, 10].

The stress relaxation of these alloys can be described by eqn. (1) as well as the stress relaxation of CuBe2 but the exponent  $n$  is higher ( $0.65 < n < 0.90$  for Nimonic PE16). The stress relaxation strength also recovers after all heat treatments. Recovery investigations at room temperature have been undertaken after cold rolling with 9% thickness reduction and subsequent annealing at 150 °C for 1 h (Fig. 4(a)). For solution-treated samples, recovery has also been investigated at room temperature and 100 °C (Fig. 4(b)). The recovery after cold rolling shows a similar time dependence as the recovery after heat treatments. The decay to equilibrium increases strongly with increasing temperature of recovery. An Arrhenius plot of recovery time constants gives activation energies between 0.45 and 0.3 eV and frequency factors between  $10^6$  and  $5 \times 10^7 \text{ s}^{-1}$ .

For step-by-step successive isochronal aging (Fig. 5) the hardness increases after the temperature region of ordered structures in the matrix. This could be due to precipitation of coarse  $M_7C_3$  [10]. At about 650 °C the precipitation of  $\gamma'$  particles begins. The fully recovered relaxation strength  $\Delta_{t \rightarrow \infty}$  in Fig. 5 shows minima at the beginning of ordering as well as at the beginning of precipitation. This means that the relaxation strength at equilibrium is lowered mostly for the smallest possible distances of dislocation pinning points. This suggests, together with the recovery and the broad spectrum of

the relaxation times (resulting from eqn. (1)), that dislocation bowing is responsible for the mean part of the measured anelastic effect. Alloy 825 has a similar composition to the matrix of Nimonic PE16. So no  $\gamma'$  precipitates can occur during heat treatment. The recovered relaxation strength of this alloy has a minimum at 350 °C (see Fig. 5). This minimum occurs at the same annealing temperature in Nimonic PE16, which can be explained by the same ordering structures in nearly the same matrix. The second minimum does not occur in Alloy 825 because no  $\gamma'$  particles can precipitate during annealing. In cold-worked Nimonic 105, maximum hardness occurs at 450 °C (Fig. 6). A minimum in the recovered relaxation strength of the same alloy is shifted to lower annealing temperatures by about 50 °C. This can be interpreted in the same way as has been done for CuBe2. More small precipitates are more effective in suppressing the bowing out of dislocations compared with the break-away of dislocations from obstacles where fewer but larger particles are more effective.

The hardness maximum (Fig. 6) cannot be due to  $\gamma'$  precipitations because 450 °C is too low a temperature for  $\gamma'$  precipitation. So it is still unknown whether the same structures in Nimonic PE16 and Alloy 825 cause the minimum in  $\Delta_{t \rightarrow \infty}$ . For solution-treated Nimonic 105, no minimum can be observed in the isochronal relaxation strength curve. This could be due to the high Co content of the alloy, lowering the solubility of Al and Ti and leading to small precipitates already during quenching.

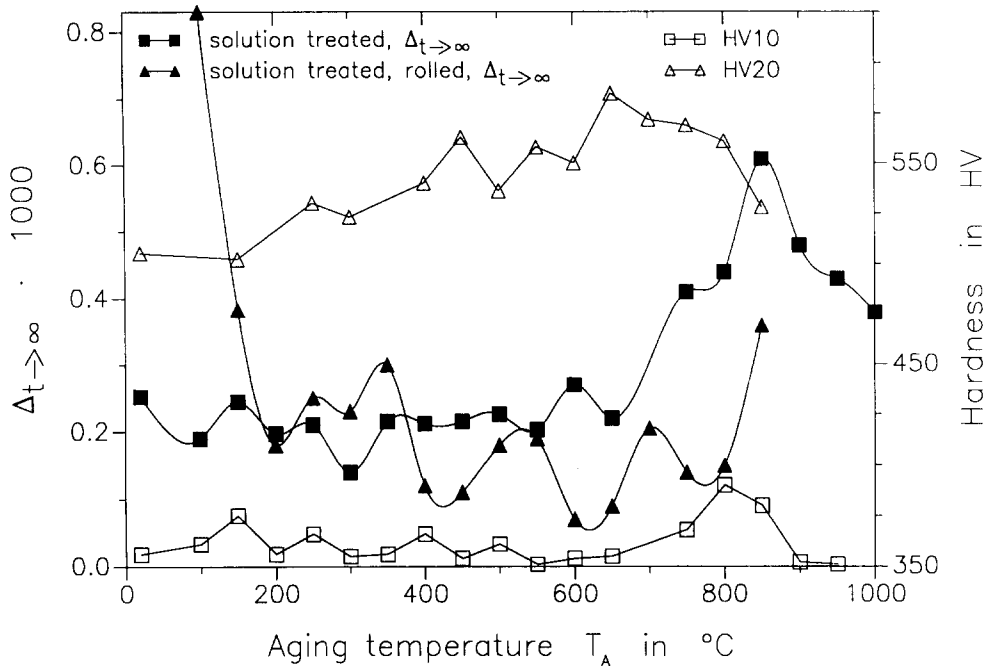


Fig. 6.  $\Delta t \rightarrow \infty$  and hardness vs. aging temperature for successive isochronal heat treatments of solution-treated and cold-worked Nimonic 105.

#### 4. Conclusions

The time dependence of stress relaxation in CuBe<sub>2</sub>, Nimonic PE16, Alloy 825 and Nimonic 105 materials can be described by a power law of the type shown in eqn. (1). This time dependence of stress relaxation is caused by a wide spectrum of relaxation times, indicating a dislocation mechanism. The investigated recovery of relaxation strength also indicates a dislocation mechanism with solid solutes. The relaxation strength is strongly influenced by the microstructure. On the assumption of a dislocation mechanism the influence of precipitates on stress relaxation strength can be explained. Relaxation effects can be suppressed to a large extent by particle sizes necessary for peak hardening or slightly smaller particles. Optimum suppression is achieved if use is made of both precipitation and ordering.

#### References

- 1 W. Riehemann, P. Fleischer and V. Martens, *Tech. Messen*, 59 (1992) 245.
- 2 W. Riehemann, P. Fleischer and V. Martens, *J. Alloys Compds.*, (1994).
- 3 K. Dies, *Kupfer und Kupferlegierungen in der Technik*, Springer, Berlin, 1967.
- 4 I. Pfeiffer, *Z. Metallkd.*, 56 (1965) 465.
- 5 H. Thomas, *Z. Metallkd.*, 52 (1961) 750.
- 6 H. Thomas, *Z. Metallkd.*, 56 (1965) 31.
- 7 J. Friedel, C. Boulanger and C. Crussard, *Acta Metall.*, 3 (1955) 380.
- 8 E. Nembach and G. Neite, *Prog. Mater. Sci.*, 29 (1985) 177.
- 9 W. Betteridge and J. Heslop, *The Nimonic Alloys*, Edward Arnold, London, 1974, p. 157.
- 10 D. Huguenin, A. Berroujji, C. Mairy, F. Vanoni and J. Hillairet, *Mater. Sci. Forum*, 15-18 (1987) 1269.
- 11 G. Schoeck, E. Bisogni and J. Shyne, *Acta Metall.*, 12 (1964) 1466.
- 12 G. Schoeck, *Acta Metall.*, 11 (1963) 617.